

Magneto-optical investigation of the noncollinear magnetic structure of gadolinium iron garnet

N. F. Kharchenko, V. V. Eremenko, S. L. Gnatchenko, L. I. Belyĭ, and É. M. Kabanova

Physico-technical Institute of Low Temperatures, Ukrainian Academy of Sciences

(Submitted July 15, 1974)

Zh. Eksp. Teor. Fiz. **68**, 1073–1090 (March 1975)

Fracture of the magnetic sublattices of gadolinium iron garnet in the vicinity of its magnetic compensation temperature $T_c = 285.5$ K is investigated. The study is carried out in both stationary and pulsed fields, with $H \parallel [111]$, by measuring the angle of rotation of the plane of polarization of linearly polarized light and measuring the change of the ellipticity of circularly polarized light. The results are discussed from the viewpoint of the three-sublattice model of the GdIG. Equations in the $H-T$ plane defining the limits of existence of collinear and skewed phases of a three-sublattice ferrite with cubic magnetic anisotropy are obtained by the molecular-field method. Approximate analytic expressions which are valid near T_c , are also obtained for the phase boundaries, for the characteristic magnetic fields, and for the temperature intervals on the phase diagrams at $H \parallel [100]$ and $H \parallel [111]$. The experimental results are compared with the calculations. The model of rigid coupling of the iron sublattices is insufficient even for a rough quantitative description of the phase boundaries of rare-earth iron garnets near T_c , and allowance must be made for the resultant noncollinearity of magnetic moments of the iron sublattices. The observed temperature and magnetic hysteresis and nonmonotonic variation of the ellipticity of circularly polarized light indicate that the magnetic structure of GdIG becomes stratified during the fracture of its sublattices.

It is known that a sufficiently strong magnetic field can disturb the collinearity of the magnetic moments of the sublattices of a ferrite. The behavior of an isotropic ferrite in a magnetic field was first considered by Tyablikov^[1] and by Gusev and Pakhomov^[2]. A confirmation of the general conclusions of the theory has been obtained in experimental investigations of rare-earth iron garnets near their magnetic-compensation temperature^[3-12], when the critical intensity of the magnetic field can be attained by usual methods, and the crystallographic-anisotropy energy is low. Comparison of the critical fields of the transition to the noncollinear phase of a magnetic system, obtained experimentally for the same iron garnets by various methods, shows that these values differ sometimes significantly (for example, in the case of gadolinium iron garnet^[7,9,10,8,9,12]). The discrepancies exceed the experimental errors. It seems that the disparities are due to the complicated character of the process of the fracture of the sublattices in real crystals and to the different sensitivities of the various experimental methods to the appearance of the noncollinear phases. The experimental results obtained for iron garnets near T_c in relatively weak magnetic fields up to 10^5 Oe are frequently compared with calculations performed in the two-sublattice-model approximation (the coupling between the iron sublattice is assumed rigid, $\lambda_{ad} = \infty$). However, allowance for the finite exchange-interaction energy between the iron sublattices can significantly alter the form of the phase diagram of the iron garnets^[9,13]. In addition, the magnetic-anisotropy energy, while small in iron garnets near T_c , leads to qualitative changes of the sublattice fracture^[14,15], and it must also be taken into account in the analysis of the canted phases and in fields greatly exceeding the anisotropy energy.

In this paper the fracture of the sublattices is investigated in gadolinium iron garnets with the aid of magneto-optical methods. The results are discussed within the framework of the molecular-field theory with allowance for the three-sublattice structure of the gadolinium

iron garnet (the coupling between the iron sublattices is not assumed to be rigid), and with allowance for its magnetic crystallographic anisotropy energy.

1. EXPERIMENTAL PROCEDURE

1. To determine the critical value of the magnetic field intensity and the temperature at which the collinear structure of the ferrite is disturbed, we make use of the fact that the optical properties of a magnetic crystal depend on the orientation of the magnetic moments of the sublattices relative to the light-propagation vector. In the general case, they depend also on the orientations of the moments relative to the crystallographic directions, and the problem of reconstructing the direction of the magnetic moment is complicated and laborious even in the case of collinear magnetic structures. However, it can be greatly simplified in special situations (predominance of one of the magneto-optical effects, small angle between the resultant optical axes in the cubic crystal). In the case of iron garnets, by selecting the rare-earth iron and the spectral region, it is possible to make the contribution of one of the sublattices predominant, so that the motion of the magnetic moment of the chosen magneto-optically active sublattice can be traced.

The simplest rare-earth iron garnets, from the optical and magnetic points of view, is the gadolinium garnet, in which the electro-dipole contribution of the gadolinium sublattices to the circular birefringence is negligible in the visible region of the spectrum. Its contribution to the linear birefringence Δn ^[16,17] is also small. Moreover, the ratio $\Delta n_{M \parallel [111]} / \Delta n_{M \parallel [100]}$ in GdIG is close to unity and the maximum angle between the optical axes is less than 13° . On the other hand, the additional change due to the fracture of the sublattice is very small, since it is determined only by the angle between the magnetic moments of the iron sublattices. The latter, at the employed magnetic-field intensities (up to 10^5 Oe), does not exceed several degrees. Thus, the gadolinium iron garnet can be roughly regarded as

an optically uniaxial crystal whose scattering characteristic is not deformed when the sublattices are fractured.

The geometry of the experiments discussed in the paper is always longitudinal—the magnetic-field intensity \mathbf{H} is collinear with a light propagation direction \mathbf{k} . The incident light has a linear or a circular polarization. We measured either the angle of rotation of the polarization plane (case of linear polarization of the incident light) or the deviation of the ellipticity of the light passing through the sample from unity (when the incident light is circularly polarized).

Rotation of the polarization plane in iron garnets in the visible region of the spectrum is due almost entirely to circular birefringence, provided only that the angle between \mathbf{k} and \mathbf{M} is not close to $\pi/2$. The maximum possible rotation angle (at $\mathbf{k} \perp \mathbf{M}$), which is due to linear birefringence, amounts to not more than several percent of the maximum (at $\mathbf{k} \parallel \mathbf{M}$) Faraday rotation, and can make a noticeable contribution only at a small value of the projection of the magnetic moment on the light propagation direction. The dependence of the Faraday angle of rotation of the polarization plane of the light on the direction of the magnetic moments of the iron-garnet sublattices can be represented in the form

$$\Phi = D(\omega)M_{1z} + A(\omega)M_{2z} + C(\omega)M_{3z} + \Phi_{\text{res}} + F(\omega)H. \quad (1)$$

Here Φ_{res} is the contribution made to the rotation by the magnetic-dipole resonant absorption in the radio-frequency and in the far infrared regions of the spectrum; M_{iz} are the projections of the magnetizations of the d, a, and c sublattices on the light propagation direction; A, D, and C are frequency-dependent proportionality coefficients between the Faraday rotation and the magnetization of the corresponding sublattices. The last term is due to the action of the magnetic field on the excited high-temperature states of the crystal. The contribution of the remaining terms in (1), for light of wavelength 6328 Å, can be characterized in order of magnitude by the values $A = -330 \text{ deg/cm-}\mu\text{B}$, $D = -190 \text{ deg/cm-}\mu\text{B}$, $C = -2.3 \text{ deg/cm-}\mu\text{B}$, $F = -2 \text{ deg/cm-kOe}$, and $\Phi_{\text{res}} = 4 \text{ deg/cm}$ ^[18]. When estimating the coefficient C, we used the results of^[19].

Confining ourselves to the three most important terms (incurring thereby at an error of less than 2%) we can write

$$\Phi = \Phi_0 \cos \theta \cos \psi + (\Phi_{10} - \Phi_{20}) \sin \theta \sin \psi + FH. \quad (2)$$

Here $\Phi_{10} = DM_1 \cos n_1 \pi$ and $\Phi_{20} = AM_2 \cos n_2 \pi$ are the spontaneous rotations of the sublattices; $n_1 = 0$ if $\mathbf{M}_1 \parallel \mathbf{k}$ and $n_1 = 1$ if $\mathbf{M}_1 \perp \mathbf{k}$; $\Phi_0 = \Phi_{10} + \Phi_{20}$ is the resultant spontaneous rotation; $\theta = \frac{1}{2}(\theta_1 + \theta_2)$, $\psi = \frac{1}{2}(\theta_2 - \theta_1)$, and θ_1 is the angle between the directions of the moments of the sublattice in the initial collinear and canted phases. In fields up to 10^5 Oe, the second term can become significant only at $\theta \approx \pi/2$, remaining small in absolute value since the angle ψ of the fracture of the iron sublattices is close to 1° . If we neglect this angle, then, measuring Φ and knowing F as well as the spontaneous rotation Φ_0 , we can determine the angle θ by which the magnetic moments of the iron sublattices deviate from the direction of the field \mathbf{H} , provided the turning of the sublattices is uniform over the sample. In any case, the decrease of the rotation, other than that due to the term FH, indicates a turning of the sub-

lattices and consequently the appearance of a noncollinear structure in the magnetic field.

Information concerning the turning of the sublattices can be obtained also from the linear birefringence. In the considered uniaxial-crystal approximation at $\mathbf{k} \parallel \mathbf{H}$, it is equal to

$$\Delta n = \Delta n_0 \sin^2 \theta. \quad (3)$$

Here Δn_0 is the spontaneous linear birefringence in a direction perpendicular to the optical axis.

2. We have measured the dependence of the angle of rotation of the light-polarization plane and of the linear birefringence in a gadolinium iron garnet as a function of the magnetic field intensity at a fixed temperature, and as a function of the temperature at a constant magnetic field. The magnetic field was produced by a pulsed or by a superconducting solenoid. The pulsed field intensity at a pulse rise time to the maximum of about 3×10^{-3} sec reached 150 kOe, while the constant field intensity was 50 kOe.

The investigated samples were mechanically polished plates of gadolinium iron garnet of approximate thickness 50μ and area up to 10 mm^2 . The sample was placed in a copper capsule, which was mounted on cold finger in a pulsed solenoid. In the stationary measurements, the capsule was placed in a cell filled with the heat-exchange gas. The temperature was measured with copper-constantan thermocouples. The absolute error in the measurement of the temperature was estimated by us at approximately $\pm 0.2^\circ\text{K}$, and the relative error at $\pm 0.1^\circ\text{K}$. The change of sample temperature under adiabatic demagnetization, in the case of pulse measurements^[7], does not exceed the experimental errors and is disregarded in the analysis of the results. The temperature gradient at the sample was monitored with thermocouples and did not exceed 0.01°K/mm . An electronic stabilizer maintained the temperature setting within $\pm 0.01^\circ\text{K}$. The temperature-scanning rates during the plotting of the temperature dependences ranged from 10^{-3} to $10^{-2}^\circ\text{K/sec}$.

The light sources were a helium-neon laser with emission wavelength 6328 Å or an incandescent lamp with a filter in the spectral region near 5800 Å.

The angle of rotation of the polarization plane was registered in the stationary measurements automatically by a null method using a Faraday cell as a compensator. The modulator was either a vibrating analyzer (polaroid film) or a Faraday cell with benzene. When working with the pulsed solenoid, the rotation was measured by an indirect double-beam method. The analyzer was a Wollaston prism. The dependence of the rotation of the plane of polarization on the magnetic field intensity was registered in the pulsed measurements with an oscillogram whose coordinates were the rotation and the field intensity. In the stationary case, we used either an x-y recorder or a single-coordinate recorder with a temperature or field marking device.

To measure the linear birefringence we used a method that has low sensitivity to circular birefringence. Its scheme is shown in Fig. 1. The circularly polarized light obtained with two phase plates underwent a change of ellipticity after passing through the birefringent sample. After passing through an analyzer rotating at a frequency Ω , the light intensity was modulated at the frequency 2Ω . The modulation depth I_{\perp}/I_{\parallel} .

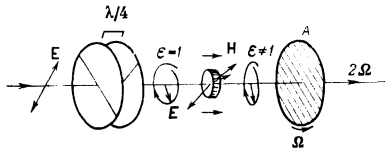


FIG. 1. System used to measure the linear birefringence.

depends on the phase shift $\Delta = (\delta^2 + 4\rho^2)^{1/2}$ between the optical modes propagating in the crystal and on the contribution $\delta = \Delta n l / \lambda$ made to it by the linear birefringence:

$$\frac{I_{\sim}}{I_{\cdot}} = \sin 2\epsilon, \quad \sin \epsilon = \frac{\delta}{\Delta} \sin \frac{\Delta}{2}. \quad (4)$$

At small angles Δ , the depth of modulation does not depend on the circular birefringence and is equal to the phase shift introduced only by the linear birefringence $I_{\sim}/I_{\cdot} = \delta$. The phase of the modulated signal is determined by the azimuth of the principal plane in the sample, as determined by the propagation vector \mathbf{k} and the optical axis. Using a reference light beam modulated by the same analyzer (not shown in Fig. 1), we can measure the azimuth of the principal plane with the aid of a phase meter.

2. EXPERIMENTAL RESULTS

1. Typical oscillograms illustrating the behavior of the Faraday rotation with increasing magnetic-field intensity at various temperatures close to T_C are shown in Fig. 2. Similar plots for the case of a stationary field are shown in Fig. 3. The rotation angle shown in Fig. 3 is the combined angle of rotation of the plane of polarization by the sample and by the windows and lenses of the optical system. The contribution made by the optical parts is shown dashed in the same figure.

We have arranged the parts of the optical system in a way as to cancel out the garnet rotation that varies linearly with the field (the term FH in (1)), whose sign is opposite to the diamagnetic rotation in the glasses of the optical system. The stray fields of the pulsed solenoid at the locations of the windows and lenses were negligible, and the measured rotation angle was close to the rotation angle of the polarization plane in the sample. The temperature dependences of the rotation of the plane of polarization and of the phase-shift angle δ due to the linear birefringence produced by turning of the sublattices are shown in Figs. 4 and 5.

Examination of Fig. 3 shows that in a certain temperature range near T_C the angle of rotation of the polarization plane in the sample does not reach its spontaneous value $\Phi_0 = \Phi(H \rightarrow 0)$, which is determined far from T_C at any field intensity. In approximately the same temperature region, the plots of the rotation against the magnetic field, in both pulsed (Fig. 2) and stationary fields (Fig. 3), reveal two characteristic singularities of the kink type at field intensities H' and H'' .

On the plots of the angle of rotation of the polarization plane against the temperature one can also separate several singularities, at which the character of the behavior of the Faraday rotation changes. Thus, after the temperature T_1 is reached, the rotation decreases with further approach to the compensation temperature. In fields exceeding 25 kOe, a distinct kink is observed at T_1 , but in fields weaker than 10 kOe, the singularity is weakly pronounced. To determine T_1 at low field inten-

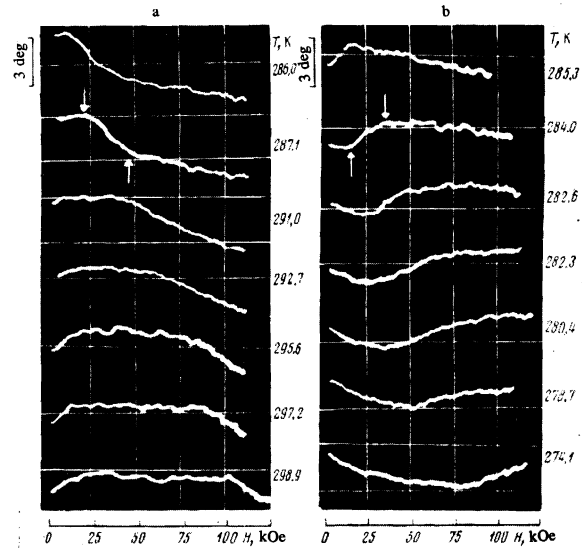


FIG. 2. Oscillograms illustrating the dependence of the Faraday rotation in gadolinium iron garnet near $T_C = 285.5^\circ\text{K}$ on the intensity of the pulsed magnetic field ($\lambda \sim 5800 \text{ \AA}$; the leading front of the magnetic field pulse was used; a) $T > T_C$, b) $T < T_C$.

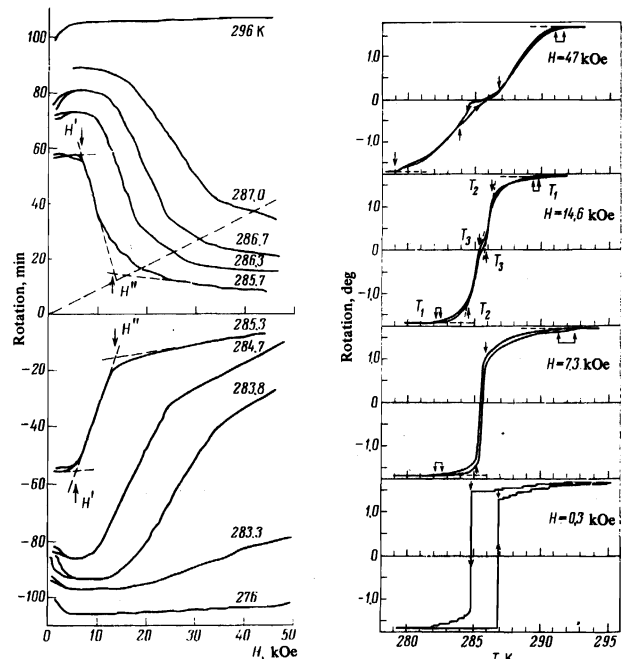


FIG. 3

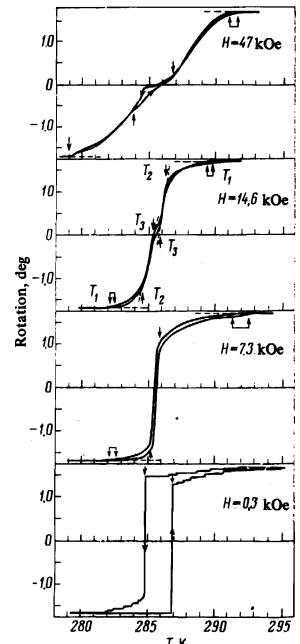


FIG. 4

FIG. 3. Behavior of Faraday rotation ($\lambda = 6328 \text{ \AA}$) in GdIG near T_C as a function of the magnetic field intensity. The dashed straight line shows the Faraday rotation of the windows of the cryostat and of the lenses of the optical system.

FIG. 4. Temperature dependences of the magnetic rotation of the polarization plane in GdIG near T_C at constant magnetic-field intensities.

sities, the sections of the $\Phi(T)$ curves closest to T_1 were replotted in logarithmic coordinates, in which they took a near-linear form. A distinct kink could be observed at the temperature T_2 , beyond which the rotation decreases rapidly. With increasing field intensity, T_2 approaches T_1 , the kink at T_2 becomes weakly pronounced and cannot be observed in fields $H > 30 \text{ kOe}$. In the immediate vicinity of T_C , starting with the temperature T_3 , an inflection of the curve is observed in fields exceeding 10 kOe. The region of the inflection broadens with increasing field intensity.

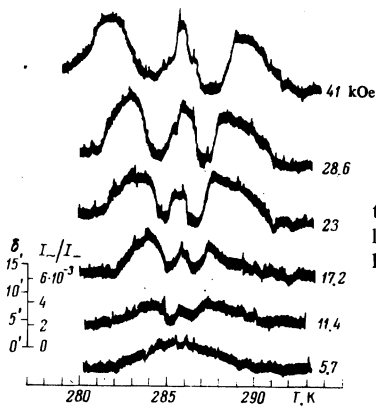


FIG. 5. Change of the ellipticity of circularly polarized light in noncollinear GdIG, $k \parallel H \parallel [111]$.

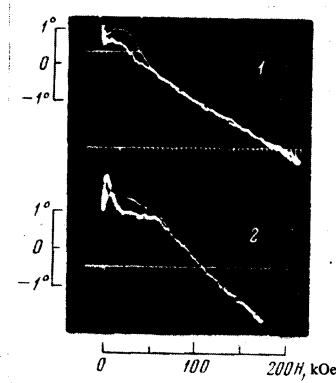


FIG. 6. Hysteresis of Faraday rotation in a pulsed magnetic field in a gadolinium iron garnet near T_c (the time during which the field builds up to the maximum is $\sim 3 \times 10^{-3}$ sec); 1) $T = 286.8$ K, 2) $T = 292.3$ K.

The temperature limits of the region of existence of linear birefringence in gadolinium iron garnet can be determined at $H \parallel k$ with a large error. Nevertheless, the obtained values of H' and T_1 agree with the corresponding values from the data of the rotation of the polarization plane. Characteristic modifications of the temperature dependence of I_{\perp}/I_{\parallel} with increasing magnetic-field intensity are shown in Fig. 5. The dips on the I_{\perp}/I_{\parallel} curves correspond to the start of the inflection region on the $\Phi(T)$ plots.

An examination of the hysteresis phenomena has revealed, in addition to the usual rectangular temperature hysteresis in weak fields of intensity up to 2.5 kOe^[8], also a temperature hysteresis of the rotation in the inflection region, and a weakly-noticeable hysteresis near the temperatures T_1 (Fig. 4). Magnetic hysteresis was observed at temperatures close to T_c in fields of intensity up to 10 kOe in the stationary case (Fig. 3) and up to 70 kOe in the case of pulsed fields (Fig. 6).

2. The decrease of the rotation in the vicinities of T_c in the magnetic field is due to turning of the sublattices, and since the turning of sublattices in a magnetic field is due to their fracture, it follows that the decrease of the rotation indicates that a noncollinear structure appears. The singularities noted on the $\Phi(H)$ and $\Phi(T)$ curves (Figs. 2–4) can be due either to changes in the plots of the turning angle after definite values of H and T are reached, or to more or less abrupt changes of the magnetic-phase concentrations in the magnetically inhomogeneous sample (for example, the appearance of a new phase), characterized by different values of the turning angle. These changes can be expected near lines where the thermodynamic stability of the magnetic configurations is lost. Therefore, by plotting on a single plane the values of H and T corresponding to the singularities separated in Figs.

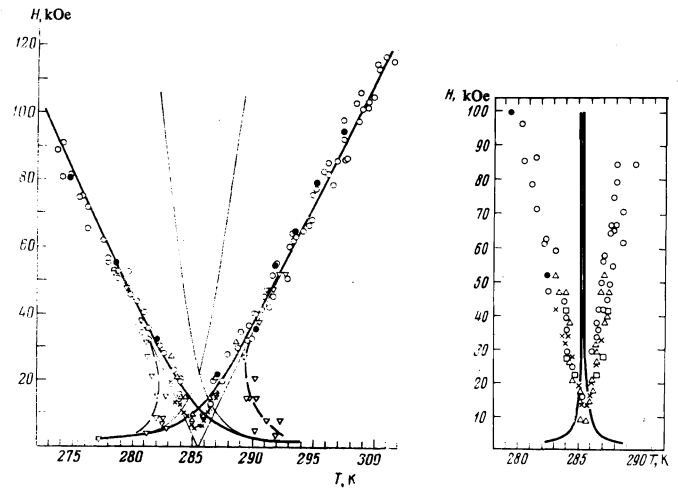


FIG. 7.

FIG. 7. Limits of the stability of collinear phases of GdIG at $H \parallel [111]$. Solid thick lines—case of three-sublattice model, calculation by formula (14) at $\beta/\alpha = 8.9$. Thin lines—case of two-sublattice model ($\lambda_{12} = \infty$, $\beta/\alpha = 33$). The experimental points were determined from the pulsed (\circ) and stationary (\times) measurements of the dependence of the Faraday rotation on the field intensity (the field H'), and from temperature measurements: ∇ — T_1 , \triangle — T_2 . The points \bullet were taken from [10].

FIG. 8. Region of inhomogeneous magnetic state in the region of reorientation of the sublattice turning plane at $H \parallel [111]$. Solid lines—calculated boundaries of the metastable phases following reorientation of the turning plane. The experimental points were determined from momentum (\circ) and stationary (\times) measurements of the dependence of the Faraday rotation on the field intensity (field H''), from the temperature measurements of the Faraday rotation (\triangle) (temperature T_3), and from the behavior of the linear birefringence (\square) (positions of the minima on the $I_{\perp}/I_{\parallel} = f(T)$ curves). The possible deviation of H from the $[111]$ direction does not exceed 5° . The points \bullet were taken from [7].

2 and 4, we obtain curves that reflect to some degree the phase diagram of the gadolinium iron garnet. Figures 7 and 8 show the results of such a combination of the singularities in the H — T plane. The points fall on certain characteristic curves, and those obtained from the temperature and field measurements are in good agreement. There is also satisfactory agreement between the results of the stationary and pulsed measurements.

There is no doubt that the characteristic features of the obtained diagram, namely, the existence of the “window” near T_c and the presence of internal lines, are connected with the magnetic anisotropy of the ferrite. On the other hand, in strong fields (stronger than 50 kOe), where the magnetic-anisotropy energy does not influence noticeably the position of the boundaries of the diagram, attention is called to the fact that the critical fields of the transition to the nonlinear phase are much weaker than those obtained from the model of rigidly coupled iron sublattices (Fig. 7). In the discussion of the applicability of this model^[4] it is customary to compare the parameters λ_{12} of the exchange interaction between sublattices a and d with the effective exchange-interaction parameter of the rare-earth sublattice with the iron sublattice $\lambda = (\lambda_{13}M_1 - \lambda_{23}M_2)(M_1 - M_2)^{-1}$, which differ noticeably from one another ($\lambda/\lambda_{12} \approx 0.1$). Naturally, a negligible change in the magnetic susceptibility of the canted phase ($\sim 10\%$), due to the finite value of λ_{12} , should cause a like change in the first critical field, provided only the sublattice magnetizations do not change in the magnetic field. But near the compensation

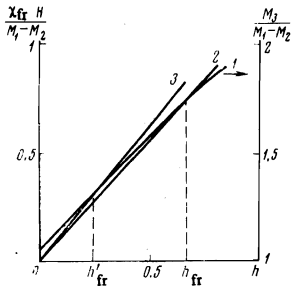


FIG. 9. Illustration of the sensitivity of the critical field of iron-garnet transition to the noncollinear state to the magnetic susceptibility of the canted phase. 1— $M_{30}(M_1 - M_2)^{-1} B_{7/2}(x)$; 2— $(\chi_{fr})^{-1} \lambda_{12} = \infty H$; 3— $1.1 (\chi_{fr}) \lambda_{12} = \infty, h = H/|\lambda(M_1 - M_2)|$.

temperature, the dependence of the magnetization of the rare-earth sublattice on the magnetic field is usually strong. In this case, even small changes of the susceptibility of the canted phase leads to appreciable changes of the critical field. Figure 9 illustrates the foregoing. In the discussion of our results we shall attempt to obtain analytic expressions that are valid near T_c in fields $H < |\lambda(M_1 - M_2)|$, taking into account the three-sublattice structure of the gadolinium iron garnet ($\lambda_{12} \neq \infty$) and its magnetic-anisotropy energy.

3. CALCULATION OF MAGNETIC PHASE DIAGRAM

1. We note that the field-induced noncollinear magnetic structure is coplanar in the absence of anisotropy. Indeed, according to the molecular-field theory, in an isotropic ferrite the magnetic moments of the sublattices are parallel to the effective field acting on them, which are equal to

$$H_i = H + \sum_{j=1}^3 \lambda_{ij} M_j, \quad i=1, 2, 3. \quad (5)$$

Taking the scalar products of both sides of the equation with the vector product $\mathbf{M}_i \times \mathbf{M}_k$, and recognizing that $\mathbf{H}_i \cdot [\mathbf{M}_i \times \mathbf{M}_k] = 0$ and that in the canted phase $\mathbf{M}_i \times \mathbf{M}_k \neq 0$ and \mathbf{H} and \mathbf{M}_j are not parallel to each other, we obtain

$$\mathbf{M}_i \cdot [\mathbf{M}_j \times \mathbf{M}_k] = 0, \quad \mathbf{H} \cdot [\mathbf{M}_i \times \mathbf{M}_k] = 0. \quad (6)$$

In a real ferrite the plane of the turning of the sublattice is determined by its magnetic-anisotropy energy. The moments can leave the plane, generally speaking, if the signs of the anisotropy constants of the individual sublattices K_i are different, or if the magnetic moments become reoriented from one easy plane to the other near T_c in the case $\mathbf{H} \parallel [111]$. However, the azimuthal angles of the moments of the sublattices should differ little from each other, since the anisotropy energy in iron garnets is much smaller than the exchange energy. In the case of a homogeneous coplanar noncollinear structure, the energy of the ferrite in the magnetic field can be written in the form

$$E = - \sum_{i=1}^3 \left[\frac{1}{2} \int_0^{H_i^{\text{exch}}} \sigma_i(x) dx + \int_{H_i^{\text{exch}}}^{H_i} \sigma_i(x) dx - K_i f(\theta_i, \varphi) \right], \quad (7)$$

$$H_i = H_i^{\text{exch}} + H \cos \theta_i = \sum_j \lambda_{ij} \sigma_j \cos(\theta_j - \theta_i) + H \cos \theta_i.$$

Here $\sigma_i = \mathbf{M}_i \cdot \mathbf{M}_i / M_i$, and φ is the azimuth of the one of the easy planes. The sublattice turning angles θ_i at which the ferrite energy is extremal are determined by the system of equations

$$\frac{\partial E}{\partial \theta_i} = - \sum_j \lambda_{ij} \sigma_j \sin(\theta_j - \theta_i) + H \sigma_i \sin \theta_i + K_i \frac{\partial f(\theta_i, \varphi)}{\partial \theta_i} = 0. \quad (8)$$

The conditions under which the system (8) can be

solved with respect to the set of angles $\{\theta_1, \theta_2, \theta_3\}$ gives the connection between the sublattice σ_i magnetizations and the field intensity H , at which the given noncollinear structure is allowed.

Let us determine first the regions of existence of collinear phases for two cases of the direction of the magnetic field—parallel to the easy axis [11] and to the difficult axis [100]. We assume that the turning angles are infinitesimally small, $\theta_i = \epsilon_i$. Expanding the trigonometric functions in series and confining ourselves to first-order terms we obtain the system of linear homogeneous equations,

$$\left\{ \sum_{j \neq i} \lambda_{ij} \sigma_j + H \sigma_i + K_i \left(\frac{\partial f(\theta_i, \varphi)}{\sin \theta_i \partial \theta_i} \right)_{\theta_i \rightarrow 0} \right\} \epsilon_i - \sum_{j \neq i} \lambda_{ij} \sigma_i \sigma_j \epsilon_j = 0, \quad i=1, 2, 3. \quad (9)$$

Equating the determinant of the system to zero, we obtain the equation

$$H^2 + \eta H^2 + \zeta H + \xi = 0, \quad (10)$$

where

$$\eta = \lambda_{12}(\sigma_1 + \sigma_2) + \lambda_{13}(\sigma_1 + \sigma_3) + \lambda_{23}(\sigma_2 + \sigma_3) + \left(\frac{K_1}{\sigma_1} + \frac{K_2}{\sigma_2} + \frac{K_3}{\sigma_3} \right) S,$$

$$\xi = (\sigma_1 + \sigma_2 + \sigma_3) (\lambda_{12} \lambda_{13} \sigma_1 + \lambda_{12} \lambda_{23} \sigma_2 + \lambda_{13} \lambda_{23} \sigma_3)$$

$$+ S \left\{ \frac{K_1}{\sigma_1} [(\lambda_{12} + \lambda_{13}) \sigma_1 + \lambda_{23}(\sigma_2 + \sigma_3)] + \frac{K_2}{\sigma_2} [(\lambda_{12} + \lambda_{23}) \sigma_2 + \lambda_{13}(\sigma_1 + \sigma_3)] \right.$$

$$\left. + \frac{K_3}{\sigma_3} [(\lambda_{13} + \lambda_{23}) \sigma_3 + \lambda_{12}(\sigma_1 + \sigma_2)] \right\} + S^2 \left(\frac{K_1 K_2}{\sigma_1 \sigma_2} + \frac{K_1 K_3}{\sigma_1 \sigma_3} + \frac{K_2 K_3}{\sigma_2 \sigma_3} \right).$$

$$\zeta = S(K_1 + K_2 + K_3) (\sigma_1 \lambda_{12} \lambda_{13} + \sigma_2 \lambda_{12} \lambda_{23} + \sigma_3 \lambda_{13} \lambda_{23}) + S^2 \{ K_1 K_2 (\lambda_{12} \sigma_1 + \lambda_{23} \sigma_2)$$

$$+ K_1 K_3 (\lambda_{12} \sigma_1 + \lambda_{23} \sigma_2) + K_2 K_3 (\lambda_{12} \sigma_2 + \lambda_{13} \sigma_3) \} + S^3 K_1 K_2 K_3, \quad S = \left(\frac{1}{\sin \theta} \frac{\partial f}{\partial \theta} \right)_{\theta \rightarrow 0}.$$

Equation (10) together with the equations for the magnetizations of the sublattices in the collinear phase

$$\sigma_i = \sigma_{i0} B_i \left(\frac{1}{kT} \mu_i \left[H + \sum_j \lambda_{ij} \sigma_j \right] \right) \quad (11)$$

delineate the regions of existence of collinear phases in a cubic three-sublattice ferrite. If there is no anisotropy and the iron sublattices are rigidly coupled ($\lambda_{12} = \infty$), then Eq. (10) takes the usual form

$$H = -\lambda(\sigma_1 + \sigma_2 + \sigma_3). \quad (12)$$

On the other hand, if λ_{12} is finite, then (10) goes over into the equation

$$H^2 + [\lambda_{12}(\sigma_1 + \sigma_2) + \lambda_{13}(\sigma_1 + \sigma_3) + \lambda_{23}(\sigma_2 + \sigma_3)] H + (\sigma_1 + \sigma_2 + \sigma_3) (\lambda_{12} \lambda_{13} \sigma_1 + \lambda_{12} \lambda_{23} \sigma_2 + \lambda_{13} \lambda_{23} \sigma_3) = 0. \quad (13)$$

which coincides with the expression (11) of [9].

It can be seen from the last equation that the intermediate collinear state is realized in an iron garnet in a strong magnetic field only if the exchange constants satisfy the relation

$$\frac{\lambda_{12}}{\lambda} \frac{1 + \lambda/\lambda_{12} + \mu_3(\lambda_{13} + \lambda_{23})/\lambda_{12}}{4\mu(1 + \mu_3 \lambda_{12} \lambda_{23} / \lambda \lambda_{12})} \geq 1,$$

$$\mu = (\sigma_1 + \sigma_2 + \sigma_3) / |\sigma_1 + \sigma_2|, \quad \mu_3 = \sigma_3 / |\sigma_1 + \sigma_2|.$$

In the case of rare-earth iron garnets at temperatures close to T_c , the cumbersome expressions (10) can be greatly simplified. Owing to the small anisotropy energy, the terms proportional to the product $K_1 K_2 K_3$ and $K_i k_j$ can be neglected. We can also disregard the anisotropy contribution to the coefficient η , since in GdIG it is smaller than the exchange contribu-

tion by several orders of magnitude. Moreover, one can neglect the anisotropic term in the expression for ζ .

We confine ourselves to the limits of the existence of the collinear magnetic structure of the iron garnet in a temperature range in the vicinity of the magnetic-compensation temperature at low magnetic field intensities, $H < |\lambda(M_1 - M_2)|$. Under these conditions we can assume that the magnetizations of the iron sublattices are constants (the resultant error does not exceed 2%), and expand the expression for the magnetization of the rare-earth sublattice (11) in powers of $h = H/\lambda(\sigma_1 + \sigma_2)$ and $t = (T - T_C)/T_C$. Inasmuch as the experimentally obtained dependence of the field of the transition of the GdIG into the canted state is close to linear if the distance to T_C is large enough, we can confine ourselves in the expansion to the linear terms in h and t and disregard in the resultant equation the terms that are higher than quadratic in h . The estimates show that the resultant contribution of the terms of higher order is insignificant to temperatures $t > 0.05$. Neglect of these terms introduces an error not larger than several percent in the determination of the critical fields. Thus, near T_C the limits of the collinear phases of the iron garnet are determined by the equation

$$h^2\alpha + ht\beta m_3' + \kappa\beta S = 0. \quad (14)$$

Here

$$\begin{aligned} \kappa &= \frac{K}{|\lambda(\sigma_1 + \sigma_2)|}, \quad K = K_1 + K_2 + K_3, \quad (14') \\ \alpha &= 1 - m_3'\beta + (\lambda - \lambda_{13} - \lambda_{23})/\lambda_{12}, \\ \beta &= 1 - \lambda_{13}\lambda_{23}/\lambda\lambda_{12}, \\ m_3' &= \frac{M_{30}}{M_1 - M_2} \left(\frac{\partial B_3(x)}{\partial x} \right)_{x=x_c}, \quad x_c = B_3^{-1} \left(\frac{M_3(T_C)}{M_{30}} \right). \end{aligned}$$

Estimating the coefficients (14') for the case of gadolinium garnets, we can conclude that the magnetic-anisotropy energy exerts a noticeable influence on the position of the boundaries at temperatures

$$t < \left| \frac{\kappa\lambda}{\lambda_{12}} S \right|^{1/2} \sim 0.01.$$

At higher temperatures, Eq. (14) yields a linear dependence

$$h = -(\beta/\alpha) m_3' t. \quad (15)$$

In rare-earth iron garnets we have $\lambda_{13}\lambda_{23} \ll \lambda\lambda_{12}$, and if the inequality $\lambda_{13}\lambda_{23}/\lambda\lambda_{12} \ll (1 - m_3')/m_3'$, is satisfied, then we can write for the critical field

$$H = - \frac{\lambda}{1 - m_3' + (\lambda - \lambda_{13} - \lambda_{23})/\lambda_{12}} M_{30} B_3'(x_c) x_c \frac{|T - T_C|}{T_C}. \quad (16)$$

Expression (16) differs from the analogous expression in the case of a model of rigidly-coupled iron sublattices in the presence of the term $(\lambda - \lambda_{13} - \lambda_{23})/\lambda_{12}$, which in iron garnets can be even larger than the term $(1 - m_3')$.

We determine now the limits of the stability of the collinear phases in the temperature region where the influence of the magnetic-anisotropy energy is significant. We consider two cases

$$a) \text{ H} \parallel [100], \quad [(1/\sin\theta)(\partial f/\partial\theta)]_{\theta=0} = 2.$$

Equation (14) has no solutions inside the temperature interval $2\Delta T_{100}^*$, the width of which is

$$2\Delta T_{100}^* = \frac{4T_C}{m_3'} \left(\frac{2\alpha\kappa}{\beta} \right)^{1/2}. \quad (17)$$

The intensity of the critical field at the edges of this

potential amounts to half the intensity obtained by extrapolating the linear dependence (16) to the temperature t^* , and is equal to

$$h^* = \left(\frac{2\beta\kappa}{\alpha} \right)^{1/2} \quad \text{or} \quad H^* = \left(\frac{2\beta}{\alpha} H_A H_{\text{exch}} \right)^{1/2}, \quad (18)$$

where $H_{\text{exch}} = \lambda(M_1 - M_2)$, $H_A = |K/(M_1 - M_2)|$.

$$b) \text{ H} \parallel [111], \quad [(1/\sin\theta)(\partial f/\partial\theta)]_{\theta=0} = -3/4.$$

Solutions exist in the entire temperature region, and at a field intensity less than

$$h_c = \left(\frac{4\beta\kappa}{3\alpha} \right)^{1/2} \quad \text{or} \quad H_c = \left(\frac{4\beta}{3\alpha} H_A H_{\text{exch}} \right)^{1/2} \quad (19)$$

there can exist both collinear phases with opposite directions of the sublattice moments.

2. Equation (14) yields the limits for the existence of the collinear phases. In a cubic ferrite, however, they may not coincide with the limits of the existence of the canted structures^[14]. To determine the region of the noncollinear phases it is convenient to express the energy of the ferrite in a magnetic field in terms of the turning angles $\theta = (\theta_1 + \theta_2)/2$ and the fracture angles

$$\psi_1 = \theta_1 - \theta, \quad \psi_2 = \theta_2 - \theta \quad (\psi_1 = \psi_2 = \psi = 1/2(\theta_1 - \theta_2))$$

of the iron sublattices and the fracture angle $\psi_3 = \theta_3 - \theta$ of the rare-earth sublattice. Minimizing the energy with respect to the angles θ , ψ , and ψ_3 , we confine ourselves to small angles ψ and ψ_3 and retain in the expansion of the trigonometric functions of these angles only the linear terms. As a result we obtain a system of three equations that are linear in ψ and ψ_3 . From the condition that the equations be compatible at a given θ , we obtain an equation relating the turning angle θ with the intensity of the magnetic field at given σ_1 , σ_2 , and σ_3 . In the general case of arbitrary anisotropy constants, the equation is cumbersome. On the other hand, taking into account the small value of the anisotropy energy in iron garnets near T_C , and neglecting its dependence on the fracture angles, we can approximately write

$$\begin{aligned} H^2 \sin\theta \cos^2\theta + H^2 \sin\theta \cos\theta [\lambda_{12}(\sigma_1 + \sigma_2) + \lambda_{13}(\sigma_1 + \sigma_3) + \lambda_{23}(\sigma_2 + \sigma_3)] \\ + H \sin\theta (\sigma_1 + \sigma_2 + \sigma_3) (\lambda_{12}\lambda_{13}\sigma_1 + \lambda_{12}\lambda_{23}\sigma_2 + \lambda_{31}\lambda_{32}\sigma_3) \\ + K \frac{\partial f(\theta, \varphi)}{\partial \theta} (\sigma_1\lambda_{12}\lambda_{13} + \sigma_2\lambda_{12}\lambda_{23} + \sigma_3\lambda_{13}\lambda_{23}) = 0. \end{aligned} \quad (20)$$

Confining ourselves, just as in the analysis of the collinear phases, to temperatures close to T_C and to weak fields, we can rewrite (20) in the form

$$h^2\alpha \sin\theta \cos\theta + ht m_3'\beta \sin\theta + \kappa\beta f/\partial\theta = 0. \quad (21)$$

We consider two cases

a) $\text{H} \parallel [001]$, in terms of coordinates $z \parallel [001]$, $x \parallel [100]$, $y \parallel [010]$ we have

$$f(\theta, \varphi) = \sin^2\theta - 7/8 \sin^4\theta - 1/8 \sin^4\theta \cos 4\varphi, \quad (22)$$

The azimuths of the easy planes are $\varphi = \pm\pi/4$. From (21) and (22) we obtain an equation $\cos\theta = r$:

$$r^3 - \frac{1}{3} \left(1 - \frac{h^2\alpha}{\kappa\beta} \right) r + \frac{m_3'}{3\kappa} ht = 0, \quad (23)$$

from which we can see that the boundaries of the canted phase coincide with the boundaries of the collinear phases, and that in the immediate vicinity of T_C there exists a region where a non-ambiguous solution of (23) is possible. Only in fields exceeding a certain critical value

$$h_c^* = \left(\frac{\beta\kappa}{\alpha} \right)^{1/2} \quad \text{or} \quad H_c^* = \left(\frac{\beta}{\alpha} H_A H_{\text{exch}} \right)^{1/2} \quad (24)$$

does a unique noncollinear structure correspond to an arbitrary temperature in the region of the canted phases.

Comparing expressions (18), (19), and (24) with one another, we see that $H_C^* : H^* : H_C = 1 : \sqrt{2} : \sqrt{4/3}$.

b) $H \parallel [111]$, in the coordinate system $z \parallel [111]$, $x \parallel [110]$, $y \parallel [11\bar{2}]$ we have

$$f(\theta, \varphi) = \frac{1}{3} \cos^4 \theta + \frac{1}{4} \sin^4 \theta - \frac{\sqrt{2}}{3} \cos \theta \sin^3 \theta \sin 3\varphi. \quad (25)$$

The turning of the sublattices in a constant magnetic field at varying temperature occurs in two planes. The reorientation of the magnetic moments from one plane to the other occurs at temperatures close to T_C . The azimuthal angles of the turning planes are respectively equal to $\pi/2$, $7\pi/6$, $11\pi/6$, and $\pi/6$, $5\pi/6$, and $3\pi/2$.

The equation for $\cos \theta$ has in this case a degree higher than cubic. The limits of the existence of canted phase determined by this equation do not agree with the limits of the collinear phases. The equation admits of three regions of metastable states, two at the edges of the diagram, where collinear and canted phases can be realized, and one at the center of the diagram, where the possible canted phases differ in the fracture angle and in the azimuth of the plane of rotation. In weak fields, they overlap each other. For phases with a turning angle exceeding a certain value, there exists a temperature "window", inside which the canted structure can be realized in an arbitrary weak field. In contrast to the case $H \parallel [001]$, collinear phases can exist in this case also in a field $H < H_C$. The width of the temperature "window" can be obtained from (21):

$$2\Delta T_{111}^*(\theta) = \frac{4T_C}{m_3} \left(\frac{z\alpha}{\beta} \operatorname{ctg} \theta \frac{\partial f}{\partial \theta} \right)^{1/2}. \quad (26)$$

The quantity ΔT_{111}^* reaches its maximum value at $\theta \approx 50^\circ$ and is close to the value $0.3\Delta T_{100}^*$.

The region of metastable states connected with the reorientation of the magnetic moments from one plane to another can be obtained from the condition $\partial^2 E(\theta, \varphi) / \partial \varphi^2 = 0$. The turning angles θ_T at which the second energy minimum appears depend on the anisotropy constants of the individual sublattices, and in the indicated approximations they are determined by the equation

$$K \cos \theta_T + [a(K_1 - K_2) + K_3] (1 - 4 \cos^2 \theta_T) h = 0, \quad (27)$$

where

$$a = \frac{1}{2} \left[\mu_1 \left(\frac{\lambda_{13}}{\lambda} - 1 \right) + \mu_2 \left(1 - \frac{\lambda_{23}}{\lambda} \right) \right] \left[\frac{\lambda_{12}}{\lambda} \mu_1 \mu_2 \left(1 - \frac{\lambda_{13} \lambda_{23}}{\lambda \lambda_{12}} \right) \right]^{-1}.$$

With the aid of (27) and (21) we can determine the limits of the region of the metastable state that differed in turning angles and azimuths of the planes where the magnetic moments are located.

4. COMPARISON OF EXPERIMENT WITH CALCULATION

1. As seen from Fig. 7, the temperature dependence of the critical field at which the noncollinear structure appears is close to linear if the distance from T_C is large enough. The slopes of the lines $H_{FR}(T)$ are somewhat different at $T > T_C$ and $T < T_C$. The mean value of $H_{FR} / |T - T_C|$ is close to 7.8 kOe/k and coincides within the limits of experimental errors with the data of [10]. From the slope $H_{FR} / |T - T_C|$, we can determine with the aid of (15) the ratio

$$\frac{\beta}{\alpha} = \frac{\mu_R}{k B_3^{-1} (M/M_{30}) |T - T_C|} \frac{H_{FR}}{T - T_C}$$

assuming that the resultant magnetization of the iron sublattices in GdIG is the same as in YIG^[20] and amounts to 22.2 cgs emu/g and that $M_{30} = 124.4 \text{ cgs emu/g}$. The obtained value $\beta/\alpha = 8.9$ can be used to determine the exchange constants λ_{13} and λ_{23} , given λ_{12} . To this end it is necessary to determine additionally the effective exchange constant $\lambda = (\lambda_{13} \sigma_1 + \lambda_{23} \sigma_2) (\sigma_1 + \sigma_2)^{-1}$ from the value of $T_C = 285.5^\circ \text{K}$ and the magnetization of the gadolinium sublattice at T_C

$$\lambda = B^{-1} \left(\frac{M}{M_{30}} \right) \frac{k T_C}{\mu_R M} = 11570 \frac{\text{Oe-g}}{\text{cgs emu}}$$

And use the temperature dependences of the magnetizations of the sublattices a and d from^[21]. Taking $\lambda_{12} = -8.08 \text{ kOe-g/cgs emu}$ ^[21], $M_1 = 75.5 \text{ cgs emu/g}$, and $M_2 = 53.3 \text{ cgs emu/g}$, we obtain $\lambda_{13} = -3250 \text{ Oe-g/cgs emu}$, and $\lambda_{23} = -1160 \text{ Oe-g/cgs emu}$. On the other hand, if we put $\lambda_{12} = -91.0 \text{ kOe-g/cgs emu}$ ^[20], then $\lambda_{13} = -3800 \text{ Oe-g/cgs emu}$ and $\lambda_{23} = -540 \text{ Oe-g/cgs emu}$.

2. To determine the boundaries of the regions of the collinear phases in fields in which an essential role is played by anisotropy energy, the width of the temperature "window" $2\Delta T^*$, and the critical fields H^* , H_C^* , and H_C , we used the obtained ratio $\beta/\alpha = 8.9$ and the anisotropy constant $K = 6.7 \times 10^3 \text{ erg/cm}^3$ obtained from^[22]. The solid lines in Fig. 7 show the obtained boundaries in the case $H \parallel [111]$. This figure shows also the boundaries of the collinear phases calculated at $\lambda_{12} = \infty$. The slope of the latter in the linear region is close to $29 \text{ kOe/}^\circ\text{K}$ and is almost four times larger than the experimental value $7.8 \text{ kOe/}^\circ\text{K}$. The calculated characteristic temperature intervals and fields of the magnetic diagram of the gadolinium garnet are listed in the table and are compared with the experimentally determined values.

The obtained width of the temperature "window" 7.6°K in the case $H \parallel [100]$ is somewhat smaller than the experimental width 9°K ^[16]. In the case $H \parallel [111]$, the difference is more significant, namely 2.3 as against 7°K . It appears that the difference between the theoretical and experimental values is due to the presence in the sample of internal local stresses. We can estimate the required stresses by starting from the relation for the magnetoelastic anisotropy energy due to the homogeneous stress^[23]:

$$E_{me} = \lambda T \sin^2 \theta.$$

Assuming that the additional broadening of the temperature "window" is approximately 5°K for $H \parallel [111]$ and is due to stresses in the plane of the plate, and assuming a magnetostriction constant $\lambda = 10^{-6}$, we obtain for the local internal stresses a value $T = 20 \text{ kg/mm}^2$ which seems feasible. The critical field H_C above which collinear phases cannot be realized at $T = T_C$ is 12 kOe (it rises to 22.5 kOe at $\lambda_{12} = \infty$). The intersection of the experimentally obtained collinear-phase boundary takes place in a field weaker than 5 kOe . It is typical that the

β/α	H_C, kOe	H_C^*, kOe	H^*, kOe	$\frac{2\Delta T_{100}^*}{K}$	$\frac{2\Delta T_{111}^*}{K}$
33 ($\lambda_{12} = \infty$)	23	20	28	2.75	0.8
8.9	12	10.3	14.6	7.6	2.3
Experiment	>5	—	20–22 [16]	9 [16]	7

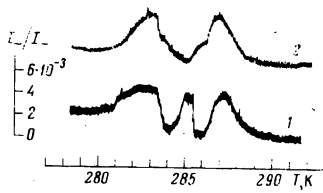


FIG. 10. Illustration of the variation of the azimuth of the sublattice turning plane: 1—change of the amplitude of the alternating signal I_{\sim} as a function of the temperature, 2—plot of I_{\sim} using a phase detector at a constant reference-signal phase. $H = 20$ kOe.

experimental points (Fig. 7) fit better the calculated curve at $|T - T_C| \gtrsim 1.5^\circ\text{K}$, and with further approach to T_C the fields at which the collinear state is no longer realized are weaker than the calculated fields at which the collinear phases become unstable. This singularity is explained by the fact that near the compensation temperature, in weak fields $H < H_C$, canted states are allowed in addition to the collinear states, and become energywise more favored before the collinear phases become unstable. The presence of energy minima for several magnetic structures should lead to a breakdown of the sample, in a narrow temperature interval near T_C , into domains with different magnetic phases. Since the magnetizations of the individual phases differ little from one another, the demagnetizing fields cannot be responsible for the formation of the domain structure. The causes for their occurrence should be analogous to those that lead to the appearance of a domain structure in antiferromagnets^[24]. An experimental confirmation of the appearance induced by the magnetic field, of a noncollinear domain structure with different magnetic phases can be the observation of temperature hysteresis on the edges and at the center of the diagram (Fig. 4) and observation of time hysteresis in a pulsed magnetic field (Fig. 6).

3. Particular interest attaches to the region of inflection on the temperature dependences of the rotation (the interval $T_3 - T_3$, Fig. 4). The boundaries of the inflection region agree well also with the singularities on the field dependences of the rotation (the fields H'' , Figs. 2 and 3). We note that the critical fields determined for GdIG by Levitin, Ponomarev, and Popov^[7], interpreted as the fields at which the ferrite goes over from the collinear to the canted state, are in much better agreement with the $H''(T)$ plots than with the boundaries of the collinear phases (Fig. 8). The change of the phase of the alternating signal when working with circularly polarized light indicates a change of the azimuth of the turning plane of the sublattice moments in a temperature range that coincides with the inflection region. Figure 10 shows $I_{\sim}(T)$ plots obtained in accordance with the scheme described above (Fig. 1), with and without the use of a phase detector. The decrease of the amplitude of the alternating signal I_{\sim} in the vicinities of T_C (Figs. 5 and 10) is attributed to the onset of an inhomogeneous magnetic structure, as a result of which the phase differences between the optical modes cancel each other. On the other hand, the increase of I_{\sim} in the immediate vicinity of T_C can be understood by taking into account the possible difference between the directions of H and $[111]$, which should give rise, at T_C , to predominantly two magnetic structures with azimuths of the sublattice turning planes that differ by an angle π .

The temperature hysteresis of the Faraday rotation, which appears in the considered temperature region, offers evidence of the presence of metastable states in

this region. However, calculation using Eqs. (21) and (27) shows that the region of metastable states that differ in turning angle and in azimuth of the turning plane of the sublattice moments should, just as in the case $\lambda_{12} = \infty$ ^[14], decrease rapidly with increasing field. It is possible that the broadening of the region of metastability is connected with the magnetoelastic energy and the presence in the sample of local stresses. But it is likewise not excluded that the inflection region is caused to a considerable degree also by domains of the magnetic-twin type, which are produced near T_C , and have the same sublattice turning angle (at the exact orientation $H \parallel [111]$) but have different turning-plane azimuths. Owing to the difference in azimuth of the optical axis relative to the light polarization plane, they can influence differently the resultant rotation of the plane of polarization and distort the $\Phi(T)$ dependence. In this case the width of the central maximum on the $I_{\sim}(T)$ curve reflects, to some degree, the width of the reorientation region. At $H = 41$ kOe, the width of the maximum is approximately 0.7°K (Fig. 5) and the temperature interval of the region of metastable states is close, according to estimates, to 0.3°K . The decrease of the width of the central maximum with increasing field intensity (28.6 and 41 kOe, Fig. 5) corresponds qualitatively to narrowing down of the metastability region.

- ¹S. V. Tyablikov, *Fiz. Met. Metalloved.* 3, 3 (1956).
- ²A. A. Gusev, *Kristallografiya* 4, 695 (1959) [*Sov. Phys.-Crystallogr.* 4, 655 (1960)]; A. A. Gusev and A. S. Pakhomov, *Izv. AN SSSR, seriya fiz.* 15, 1327 (1961).
- ³N. F. Kharchenko, V. V. Eremenko, and L. I. Belyi, *Zh. Eksp. Teor. Fiz.* 55, 419 (1968) [*Sov. Phys.-JETP* 28, 219 (1969)].
- ⁴A. E. Clark and E. Gallen, *J. Appl. Phys.*, 39, 5972 (1968).
- ⁵K. P. Belov, R. Z. Levitin, B. K. Ponomarev, and Yu. F. Popov, *ZhETF Pis. Red.* 10, 13 (1969) [*JETP Lett.* 10, 8 (1969)].
- ⁶K. P. Belov, L. A. Chernikova, E. V. Talalaeva, R. Z. Levitin, T. V. Kudryavtseva, S. Amadezi, and V. N. Ivanovskii, *Zh. Eksp. Teor. Fiz.* 58, 1923 (1970) [*Sov. Phys.-JETP* 31, 1035 (1970)].
- ⁷R. Z. Levitin, B. K. Ponomarev, and Yu. F. Popov, *Zh. Eksp. Teor. Fiz.* 59, 1952 (1970) [*Sov. Phys.-JETP* 32, 1056 (1971)].
- ⁸E. L. Smirnova, V. I. Smirnov, and Yu. I. Ukhonov, *Izv. AN SSSR, seriya fiz.* 25, 1186 (1971); *ZhETF Pis. Red.* 11, 435 (1970) [*JETP Lett.* 11, 293 (1970)].
- ⁹J. Bernasconi and D. Kuse, *Phys. Rev.*, B3, 811 (1971).
- ¹⁰G. Fillon, G. Hug, and C. R. Paris, 271, B1045 (1970).
- ¹¹J. L. Feron, G. Fillon, and G. Hug, *Zs. Angew. Phys.* 32, 219 (1971).
- ¹²O. A. Grzhegorzhevskii and R. V. Pisarev, *Zh. Eksp. Teor. Fiz.* 65, 633 (1973) [*Sov. Phys.-JETP* 38, 312 (1974)].
- ¹³J. L. Feron, G. Fillon, and G. Hug., *J. Phys.*, 34, 247 (1973).
- ¹⁴A. K. Zvezdin and V. M. Matveev, *Zh. Eksp. Teor. Fiz.* 62, 260 (1972) [*Sov. Phys.-JETP* 35, 140 (1972)].
- ¹⁵R. Alben, *Phys. Rev.*, B2, 2767 (1970).
- ¹⁶R. V. Pisarev, I. G. Sini, N. N. Kolpakova, and Yu. M. Yakovlev, *Zh. Eksp. Teor. Fiz.* 60, 2188 (1971) [*Sov. Phys.-JETP* 33, 1175 (1971)].

- ¹⁷J. F. Dillon and J. P. Remeika, *J. Appl. Phys.*, **41**, 4613 (1970).
¹⁸N. F. Kharchenko and V. V. Eremenko, in: *Fiz. kond. sost.*, Khar'kov, FTINT AN UkrSSR **4**, 144 (1969).
¹⁹Y. R. Shen and N. Bloembergen, *Phys. Rev.*, **133**, A515 (1964).
²⁰E. E. Anderson, *Phys. Rev.*, **134**, A1581 (1964).
²¹J. D. Lister and G. B. Benedek, *J. Appl. Phys.*, **37**, 1330 (1966).

- ²²G. P. Podrigue, H. Meyer, and R. V. Jones, *J. Appl. Phys.*, **31**, 3765 (1960).
²³C. Kittel, *Rev. Mod. Phys.*, **21**, 511 (1949).
²⁴M. M. Farztdinov, *Usp. Fiz. Nauk* **84**, 611 (1964) [*Sov. Phys.-Uspekhi* **7**, 855 (1965)].

Translated by J. G. Adashko
115